

论 著

婴儿型纤维肉瘤的MR表现和Ki67表达分析

刘长林¹ 丁宇¹ 李晓燕¹
曾凡勇¹ 储彩婷² 李文华^{1,2,*}

1.新华医院崇明分院医学影像科(上海202150)
2.上海交通大学医学院附属新华医院放射科(上海202150)

【摘要】目的 探讨婴儿型纤维肉瘤(IFs)的MR表现特点和Ki67的表达状态。**方法** 对11例经手术病理证实的IFs的MR资料进行回顾性分析,对其发生的部位、大小、边界、形态、信号特点、表观弥散系数(ADC)值和强化特征及Ki67表达程度进行研究分析。**结果** 11例患者中,头颈部3例,肢体7例(上肢前臂3例,上臂1例;下肢腓窝区1例,小腿1例),腹膜后起源1例。肿瘤大小从0.7×1.1×1.2cm到3.0×7.0×9.0cm。11例肿瘤边界规则,呈实性者7例,囊实性者4例。肿瘤实性部分T₁WI呈等或稍低信号,T₂WI和弥散加权成像(DWI)呈高信号,肿瘤实性部分ADC值范围为0.75~1.12mm²/s。增强后肿瘤实性部分和囊壁呈明显强化。Ki67的表达程度为15%~30%(21.73±6.08%)。**结论** 婴儿型纤维肉瘤为好发于肢体和头颈部的边界清楚的实性或囊实性肿块,增强后实性部分显著强化,肿瘤Ki67呈低-中表达是其特征。

【关键词】 婴儿; 婴儿型纤维肉瘤; 磁共振成像; 表观弥散系数; Ki67

【中图分类号】 R445.2

【文献标识码】 A

DOI:10.3969/j.issn.1672-5131.2023.02.057

Comparisons of MR Features and Ki67 expressions in Patients with Infantile Fibrosarcomas

LIU Chang-lin¹, DING Yu¹, LI Xiao-yan¹, ZENG Fan-Yong¹, CHU Cai-ting², LI Wen-hua^{1,2,*}.

1. Department of Medical Imaging, Xinhua Hospital Chongming Branch, Shanghai 202150, China

2. Department of Radiology, Xinhua Hospital Affiliated to Shanghai Jiao Tong University School of Medicine, Shanghai 200092, China

ABSTRACT

Objective To explore MRI appearances and the expression of Ki67 of infantile fibrosarcomas (IFs). **Methods** The MR data and the expression of Ki67 of 11 patients of histopathologically proven IFs were retrospectively reviewed. The sites, size, border, morphology, imaging features, and apparent diffusion coefficient (ADC) value of lesions were measured and analyzed. **Results** Of 11 IFs, the masses arisen on head and neck in 3 cases, the limbs in 7 (including 3 cases in the forearm of upper limbs, 1 case in the upper arm), 1 in the popliteal fossa of lower extremity, 1 in the calf and 1 in the retroperitoneal region. The ranges in size for the lesions were from 0.7×1.1×1.2cm~3.0×7.0×9.0cm. 11 tumors were all well-defined and 7 was solid and 4 was solid-cystic. The solid components of all tumors were isointensity or slight hypointensity compared to muscle on T₁-weighted images and hyperintensity on T₂-weighted images and DW imaging with a range of mean ADC value from 0.75~1.12mm²/s. The solid component and cystic wall of the tumors were strong enhancement after administration of contrast medium. The range of expression of Ki67 was 15%~30%(21.73±6.08%). **Conclusion** IFs were predominantly occurred in limbs and head and neck. The tumor maybe solid or solid-cystic with well-defined margins. The characteristics of MR imaging of IF were isointensity or slight hypointensity to muscle on T₁-weighted images and hyperintensity on T₂-weighted images with strong enhancement of solid components and low to intermediate expression of Ki67.

Keywords: Infants, Infantile Fibrosarcomas, Magnetic Resonance Imaging, Ki67

婴儿型纤维肉瘤(infantile fibrosarcomas, IFs)又称先天性婴儿型纤维肉瘤(congenital infantile fibrosarcomas, CIFs)或先天性纤维肉瘤(congenital fibrosarcoma, CFs), IFs为相对少见的儿童期软组织肿瘤,约占儿童期全部恶性肿瘤的1~2%和婴儿期软组织恶性肿瘤的12%及儿童期纤维母细胞性和肌纤维母细胞性肿瘤的13%^[1-5]。尽管IFs组织学上和成年人发生的经典型纤维肉瘤相同,但生物学上IFs却截然不同于前者,IFs肿瘤很少发生转移、手术切除后复发率低、预后远远好于成年性纤维肉瘤。

我们对11例资料完整,均经手术病理和肿瘤基因检测证实的婴儿型纤维肉瘤的MR影像学及Ki67表达资料进行回顾性分析研究,现进行报道。

1 资料与方法

1.1 患者资料 收集2012年8月至2020年6月间,临床资料完整,均经手术病理和肿瘤基因检测证实的11例婴儿型纤维肉瘤的MR资料(其中1例有CT平扫检查)影像学资料,包括发病年龄、发生的部位、大小、边界、形态、信号特点、表观弥散系数(ADC)值和强化特征和Ki67表达程度进行回顾性分析研究。11例患者中,男性6例,女性5例;发病年龄最小者5周(该患者出生前胎儿畸形筛查即发现右侧头颈部肿块),最大者2岁。全部患儿均无明显症状,皆为患儿父母发现肿块或肢体局部增粗就诊。11例患者均进行手术或扩大根治性手术切除肿瘤并随访,均无复发。

1.2 MR设备和技术参数 使用GE Signal 1.5T和3.0T超导磁共振机,行横断面T₁WI(TR 400~600ms, TE 10~14ms)和T₂WI-FS(TR 4000~6000ms, TE 100~120ms)、矢状面或冠状面T₂WI (TR 3000~6000ms, TE 100~110ms),层厚5mm,间隔1mm,视野(FOV)15~30cm,矩阵256×256,激励次数为2。DWI成像采用单激发平面回波成像序列(TR 8000~10000ms, TE 70~100ms),行横轴位成像,按各向同性施加扩散敏感梯度磁场,b值取0、1000s/mm²,层厚5mm,间隔1mm,视野15~30cm,矩阵256×128,激励次数为2次。增强对比剂选用钆喷酸葡胺(Gd-DTPA),注射剂量为0.1mmol/kg体重,注射对比剂后行横断面及矢状面或冠状面T₁WI扫描。

1.3 ADC测量 病灶ADC值的测量:在GE后处理工作站上自动生成ADC图,将感兴趣区(Region of interest, ROI)放置于病灶实性部分,对照T₁WI、T₂WI及增强图像,避免囊变、坏死及血管区域和化学位移伪影等区域,ROI范围约6mm²~20mm²,每个病灶测量3次不同实性区域并取平均值作为ADC值(ADCmean)。

1.4 Ki67免疫组织化学检查 将石蜡包埋的组织标本块切成3~4μm切片,切片去石蜡化,在柠檬酸盐缓冲液(0.01mol/L, pH6.0)中熔融,放入微波炉(98℃)中20分钟。然后取出浸泡在缓冲液中的溶液,冷却20分钟,用3%的过氧化氢处理5分钟。所有病例均行1/100稀释率的抗p53(p53-DO7-L-CE)和Ki67(MIB-1)抗体。Ki67染色:细胞核内棕黄色颗粒的细胞为阳性细胞,计数10个高倍视野(×400)阳性细胞。

【第一作者】 刘长林,男,主治医师,主要研究方向:骨肌系统疾病。E-mail: 258055617@qq.com

【通讯作者】 李文华,男,主任医师,主要研究方向:儿童和妇科肿瘤影像学。E-mail: wenhualimd@126.com

2 结果

11例患者中, 3例起源于头颈部, 见图1, 7例起源肢体, 其中上肢前臂3例, 见图2, 上臂1例, 下肢腓窝区1例, 小腿1例和腹膜后1例。11例患者均进行手术或扩大根治性手术切除肿瘤, 组织病理学及分子检测 ETV6-NTRK3融合基因阳性, SMA(-), DES(-), CD34(-), CD31(+), STAT6(-)等指标确立诊断。11例肿瘤大小从 $0.7 \times 1.1 \times 1.2 \text{cm}$ - $3.0 \times 7.0 \times 9.0 \text{cm}$, 呈实性者7例, 囊实性者4例, 全部边界清晰规则, 对邻近结构无明显浸润, 其

中1例CT和MRI显示尽管肿瘤巨大, 肿瘤仅推压邻近颅骨而不破坏颅骨。肿瘤实性部分 $T_1\text{WI}$ (与邻近正常肌肉对比)呈等或稍低信号, $T_2\text{WI}$ 呈高信号; 弥散加权成像(DWI)呈高信号和ADC图呈低信号, 表明肿瘤组织内水分子弥散明显受限, 肿瘤实性部分ADC值范围为 $0.75 \sim 1.12 \text{mm}^2/\text{s}$ 。增强后肿瘤实性部分呈明显强化, 囊壁部分强化程度低于实性部分的强化程度。11例患者中, Ki67阳性表达程度为15%~30%, 均值为 $21.73 \pm 6.08\%$ 。

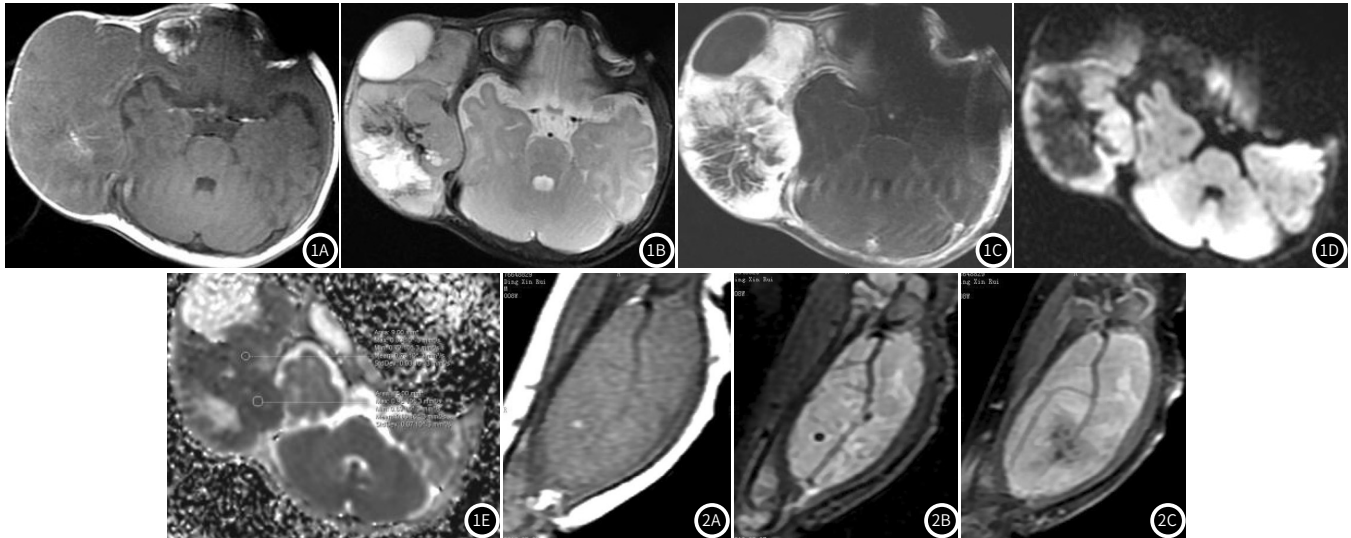


图1 右侧头颈部婴儿型纤维肉瘤。图1A: 横断面 $T_1\text{WI}$ 显示肿瘤呈等信号。图1B: 横断面 $T_1\text{WI}$ 肿瘤呈囊实性, 实性成分与头皮软组织比较呈稍高信号。图1C: 横断面增强 $T_1\text{WI}$ 显示肿瘤呈明显强化, 肿瘤实质内可见强化减弱的纤维成分, 肿瘤推压颞骨和脑膜而未侵入颅内。图1D: 横断面DWI显示肿瘤实质成分呈高信号。图1E: 肿瘤横断面ADCMap上实质成分呈低信号, 表现水分子弥散受限。图2 右前臂(男, 8周)IFs。图2A: 冠状面 $T_1\text{WI}$ 显示肿瘤呈等信号。图2B: 冠状面 $T_2\text{WI}$ 显示肿瘤(与肌肉比)呈高信号, 肿瘤内可见流空的血管。图2C: 冠状面增强 $T_1\text{WI}$ 显示肿瘤呈明显强化。横断面DWI显示肿瘤呈高信号。

3 讨论

婴儿型纤维肉瘤(IFs)为纤维母细胞性和肌纤维母细胞性肿瘤的一个亚型, 是一类起源于间充质细胞, 主要由恶性纤维母细胞构成的恶性肿瘤。文献也曾报道其为幼年性纤维肉瘤(juvenile fibrosarcoma)、婴儿髓样纤维瘤病(medullary fibromatosis of infancy)、侵袭性婴儿纤维瘤病(aggressive infantile fibromatosis)、婴儿促结缔组织增生性纤维肉瘤(desmoplastic fibrosarcoma of infancy)等^[4-6], IFs或CIFs为一种相对少见的儿童期非横纹肌性软组织低级别恶性肿瘤, 约占儿童期全部恶性肿瘤的1-2%, 占婴儿期软组织恶性肿瘤的12%及儿童期纤维母细胞性和肌纤维母细胞性肿瘤的13%^[1-6]。该肿瘤的发生发展可能与染色体平衡易位(t(12;15)(p13;q25), 使位于12p13的ETV6与15q25神经生长酪氨酸激酶受体3(NTR3)融合, 形成的ETV6/NTR3融合基因激活肿瘤的下游和生长通路有关, 同时ETV6-NTR3融合基因表达也是组织病理学上IFs区别于儿童纤维母细胞/肌纤维母细胞和成人型纤维肉瘤的特异性指标^[4-6]。文献报道绝大多数IFs发现时年龄小于2岁, 其中小于1岁者占80%以上^[1-8], 男性发病率略高于女性, 而且研究发现IFs尽管和经典成人型纤维肉瘤有相近的组织学特征, 但IFs没有明显的侵袭性, 肿瘤完全切除后复发率低、预后好, 10年生存率高达80%~90%。我们的11例患者中, 术后随访均未见复发及转移, 其中1例随访时间接近6年未见复发迹象。

IFs可发生于全身的任何部位, 又以肢体为常见部位, 约占IFs起源部位的70%以上, 我们的11例资料中, 7例(66.7%)起源于四肢, 肿瘤多位于皮下或肌间, 这其中, 下肢多于上肢, 远端多于近端, 其次为头颈部, IFs很少发生于躯干, 与文献报道一致^[1-14]。

IFs的影像学表现与其他软组织肿瘤的表现具有一定的相似性, 文献总结没有特异性的影像学诊断特征^[3,15]。我们的11例资料显示, 除1例右侧眼眶外皮皮下肿瘤较小外, 其余10例发现时均为较大软组织肿块, 肿瘤为实质性, 4例肿瘤呈囊实性肿块。与邻近的肌肉比较, 肿瘤于 $T_1\text{WI}$ 上呈等或略低信号, $T_2\text{WI}$ 和DWI上呈高信号, 肿瘤边界清晰、推压而不侵犯邻近结构, 增强后肿瘤实性成分呈明显强化或许是IFs(除发病年龄外)具有一定诊断价值的影像学特点, 此外肿瘤内形成过多或明显纤维组织时, 可导致肿瘤内该区域强化减弱或导致非均匀性强化。文献报道IFs血管造影

为血供丰富, 这与我们MRI资料上肿瘤呈明显强化一致^[3,8]。

IFs需同婴幼儿期发生的血管瘤、血管外皮细胞瘤、横纹肌肉瘤、肌纤维母细胞瘤等肌纤维母/肌纤维母细胞肿瘤类肿瘤鉴别。血管瘤可与IFs一样于出生时即存在或于生后发生, 在1~2岁内有快速生长的过程, MRI增强呈明显强化肿块, 尽管血管瘤强化可存在不均匀性, 但 $T_2\text{WI}$ 上呈明显高信号, 很少有较大坏死或许不同于IFs, 其次血管瘤触诊呈柔软性肿块, 而IFs呈坚硬肿块也有助于两者的鉴别。IFs与肌纤维母细胞瘤的临床表现具有相似性, 但肌纤维母细胞瘤以头颈及躯干为好发部位, 发生于肢体者少于IFs, 无论是单发(孤立)性或多中心性肌纤维母细胞瘤, 典型呈乏血供肿瘤且易发生中央坏死而不同于IFs呈明显富血供肿瘤的特点。MRI表现上, IFs与血管外皮细胞瘤、横纹肌肉瘤或其他软组织肿瘤的表现具有相似性, 鉴别困难, 甚至IFs与其他纤维类良、恶性肿瘤如成人型纤维肉瘤等组织学也具有相似性和难以鉴别, 分子生物学检查ETV6-NTRK3表达对IFs具有一定的特异性, 也是同其他具有类似组织学特征的软组织肿瘤的鉴别点, 再结合SMA(-)、DES(-)、CD34(-)等指标可最终确立诊断^[4-13]。

Ki67是目前最能反映细胞增生的核抗原标记物, 其表达的程度与多种肿瘤的发生、发展、转移和预后密切相关。越来越多的研究证明它的高表达往往预示肿瘤预后差、易于转移和术后复发。尽管目前仍没有一个国际统一的Ki67阈值标准, 可准确用于独立判断不同肿瘤患者的临床转归, 也没有一个Ki67表达的高低程度范围用于判断IFs的生物学行, 但依据Ki67的表达程度, 将其分为低表达($\leq 15\%$), 中表达(16%~30%)和高表达($> 30\%$)。而且, 一项对64196例乳腺癌Ki67表达的meta(荟萃)分析显示, 当用Ki67表达 $> 25\%$ 时, 可以作为一独立指标用于乳腺癌总体生存率的预判。本组11例IFs患儿中, 仅3例Ki67表达大于25%, 提示肿瘤细胞增生的活跃程度并不高, Ki67的总体低表达也是IFs患者预后比较好的一个可参考指标^[14-16]。

总之, IFs是以发生于婴儿, 出生即存在或于2岁内尤其是1岁内出现肢体或其他部位肿块, 肿块生长快, 血供丰富, 很少破坏邻近结构和发生转移是其比较具有诊断价值的表现。

(下转第 177 页)

- evaluation of normal tissues and head and neck cancer using dual-energy CT[J]. AJNR Am J Neuroradiol, 2015, 36 (8): 1518-1524.
- [5]李琦, 罗天友, 吕发金, 等. 能谱CT定量分析在确定非小细胞肺癌病理类型中的价值[J]. 中华放射学杂志, 2017, 51 (4): 257-261.
- [6]郑星星, 冯峰, 丁勇生, 等. 双源能谱CT虚拟平扫替代常规平扫评估食管癌的可行性研究[J]. 国际医学放射学杂志, 2020, 43 (2): 150-155.
- [7]李琦. 双源CT双能双期增强扫描在食管癌诊断中的应用价值[D]. 河北医科大学, 2013.
- [8]秦洪涛. 双能双期增强CT对食管癌诊断价值的初步评价[D]. 河北医科大学, 2011.
- [9]Guo X, Meng X, Liu R. Prognostic value of microvessel density in esophageal squamous cell carcinoma—a systematic review and meta-analysis. Pathol Res Pract, 2021, 227: 153644.
- [10]夏振元. 双能量CT成像标准化碘浓度评估食管癌T分期的可行性[D]. 广西医科大学, 2017.
- [11]Griffin J M, Reed C E, Denlinger C E. Utility of restaging endoscopic ultrasound after neoadjuvant therapy for esophageal cancer[J]. Ann Thorac Surg, 2012, 93 (6): 1855-1860.
- [12]李弋, 叶兆祥. 双能CT成像在直肠癌术前分期评估中的应用进展[J]. 国际医学放射学杂志, 2020, 43 (2): 211-213, 218.
- [13]Zhou Y, Liu D, Hou P, et al. Low-dose spectral insufflation computed tomography protocol preoperatively optimized for T stage esophageal cancer – preliminary research experience[J]. World J Gastroenterol, 2018, 24 (36): 4197-4207.
- [14]李佳音, 梁盼, 高剑波, 等. DECT碘参数在不同分化胃腺癌中的诊断价值[J]. 实用放射学杂志, 2017, 33: 754-757.
- [15]Shi C, Zhang H, Yan J, et al. Decreased stage migration rate of early gastric cancer with a new reconstruction algorithm using dual-energy CT images: a preliminary study[J]. Eur Radiol, 2017, 27: 671-680.
- [16]缪琪, 任克. 能谱CT在胰腺癌诊断和治疗中的应用进展[J]. 中国医学影像技术, 2016, 32 (1): 142-145.
- [17]赵海波, 林盛才. 能谱CT在肝癌中的应用研究进展[J]. 中华灾害救援医学, 2019, 7 (6): 352-356.
- [18]Pellat A, Dohan A, Soyer P, et al. The role of magnetic resonance imaging in the management of esophageal cancer. Cancers (Basel), 2022, 14 (5): 1141.
- [19]尹春国, 韩久付, 蔡宝坡. 食管癌不同区域淋巴结转移特征及CT诊断效能[J]. 现代仪器与医疗, 2018, 24 (2): 5-7.
- [20]Kim T J, Kim H Y, Lee K W, et al. Multimodality assessment of esophageal cancer: preoperative staging and monitoring of response to therapy[J]. Radiographics, 2009, 29 (2): 403-421.
- [21]Rizzo S, Radice D, Femia M, et al. Metastatic and non-metastatic lymph nodes: quantification and different distribution of iodine uptake assessed by dual-energy CT[J]. Eur Radiol, 2018, 28 (2): 760-769.
- [22]Sun X, Niwa T, Ozawa S, et al. Detecting lymph node metastasis of esophageal cancer on dual-energy computed tomography. Acta Radiol, 2022, 63 (1): 3-10.
- [23]Megibow A J, Kambadakone A, Ananthakrishnan L. Dual-energy computed tomography: image acquisition, processing, and workflow[J]. Radiol Clin North Am, 2018, 56 (4): 507-520.
- [24]Rizzo S, Radice D, Femia M, et al. Metastatic and non-metastatic lymph nodes: quantification and different distribution of iodine uptake assessed by dual-energy CT[J]. Eur Radiol, 2018, 28 (2): 760-769.
- [25]Sato K, Morohashi H, Tsumihama F, et al. Dual energy CT is useful for the prediction of mesenteric and lateral pelvic lymph node metastasis in rectal cancer[J]. Mol Clin Oncol, 2019, 10 (6): 625-630.
- [26]Tawfik A M, Razeq A A, Kerl J M, et al. Comparison of dual-energy CT-derived iodine content and iodine overlay of normal, inflammatory and metastatic squamous cell carcinoma cervical lymph nodes[J]. Eur Radiol, 2014, 24 (3): 574-580.
- [27]卫军, 马宣传. 能谱CT成像定性评估不同分化食管癌转移淋巴结的应用价值[J]. 蚌埠医学院学报, 2021, 46 (1): 25-28, 32.
- [28]丁聪, 余莹莹, 文智. 能谱CT在食管癌转移性淋巴结诊断中的应用价值[J]. 山东医药, 2018, 58 (22): 41-43.
- [29]王全来, 温平贵, 王峰. 宝石能谱CT成像技术对食管癌术前分期的临床价值[J]. 中国CT和MRI杂志, 2019, 17 (3): 33-35+108.
- [30]周胜利, 陈伟, 柏根基, 等. 双能量CT及DWI食管癌病理分级对照[J]. 放射学实践, 2020, 35 (6): 746-749.
- [31]贾鑫鑫, 程涛. CT能谱成像评估食管鳞癌的分化程度[J]. 中国医学影像学杂志, 2014, 22 (8): 602-606.
- [32]傅昭昭, 蔡志奇, 周志明, 等. 不同分化程度食管鳞癌的能谱CT参数特征及其诊断效能[J]. 世界华人消化杂志, 2017, 25 (33): 2967-2972.
- [33]刘月华, 朱绍成, 史大鹏, 等. CT能谱成像术前评估食管鳞状细胞癌病理分级的临床价值[J]. 中华医学杂志, 2017, 97 (43): 3406-3411.
- [34]Cheng SM, Ling W, Zhu J, et al. Dual energy spectral CT imaging in the assessment of gastric cancer and cell proliferation: a preliminary study[J]. Sci Rep, 2018, 8 (1): 17619.
- [35]原士超, 赵庆, 范红燕. 双能CT对胃间质瘤中Ki-67表达的预测价值及其与病理参数的关系[J]. 临床荟萃, 2021, 36 (11): 1013-1018.
- [36]Fan S, Li X, Zheng L, et al. Correlations between the iodine concentrations from dual energy computed tomography and molecular markers Ki-67 and HIF-1 α in rectal cancer: A preliminary study[J]. Eur J Radiol, 2017, 96: 109-114.
- [37]Dou P, Liu Z, Xie L, et al. The predictive value of energy spectral CT parameters for assessing Ki-67 expression of lung cancer[J]. Transl Cancer Res, 2020, 9 (7): 4267-4278.
- [38]Wang X, Liu D, Zeng X, et al. Dual-energy CT quantitative parameters for evaluating immunohistochemical biomarkers of invasive breast cancer[J]. Cancer Imaging, 2021, 21 (1): 4.
- [39]Zhang L J, Wu S, Wang M, et al. Quantitative dual energy CT measurements in rabbit VX2 liver tumors: Comparison to perfusion CT measurements and histopathological findings[J]. Eur J Radiol, 2012, 81 (8): 1766-1775.
- [40]Chen XH, Ren K, Liang P, et al. Spectral computed tomography in advanced gastric cancer: Can iodine concentration non-invasively assess angiogenesis? [J]. World J Gastroenterol, 2017, 23 (9): 1666-1675.
- [41]Ge X, Yu J, Wang Z, et al. Comparative study of dual energy CT iodine imaging and standardized concentrations before and after chemoradiotherapy for esophageal cancer[J]. BMC Cancer, 2018, 18 (1): 1120.
- [42]Fehrenbach U, Feldhaus F, Kahn J, et al. Tumor response in non-small-cell lung cancer patients treated with chemoradiotherapy—Can spectral CT predict recurrence? [J]. J Med Imaging Radiat Oncol, 2019, 63: 641-649.
- [43]Kruis M F. Improving radiation physics, tumor visualisation, and treatment quantification in radiotherapy with spectral or dual-energy CT [J]. J Appl Clin Med Phys, 2022, 23 (1): e13468.

(收稿日期: 2022-10-18)

(校对编辑: 姚丽娜)

(上接第 170 页)

参考文献

- [1]Nagasubramanian R, Wei J, Gordon P, et al. Infantile Fibrosarcoma With NTRK3-ETV6 Fusion Successfully Treated With the Tyrosine Kinase Inhibitor LOXO-101. Pediatr Blood Cancer, 2016, 63 (8): 1468-1470.
- [2]Kim H Y, Cho Y H, Byun S Y, et al. A case of congenital infantile fibrosarcoma of sigmoid colon manifesting as pneumoperitoneum in a newborn. J Korean Med Sci [J], 2013, 28 (1): 160-163.
- [3]Canale S, Vanel D, Couanet D, et al. Infantile fibrosarcoma: Magnetic resonance imaging findings in six cases [J]. Eur J Radiol, 2009, 72 (1): 30-37.
- [4]Parida L, Fernandez-Pineda I, Uffman J K, et al. Clinical management of infantile fibrosarcoma: A retrospective single-institution review. Pediatr Surg Int, 2013, 29 (7): 703-708.
- [5]Zeytun H, Okur M H, Basuguy E, et al. Congenital-infantile fibrosarcoma of the ileocecal region: The first case presentation [J]. Pediatr Surg Int, 2016, 32: 97-99.
- [6]Muzumdar D, Michaud J, Ventureyra E C. Primary giant congenital infantile fibrosarcoma of the scalp: Case report and review of literature [J]. Childs Nerv Syst, 2006, 22: 300-304.
- [7]Lopes R N, Alves Fde A, Rocha A C, et al. Head and neck solitary infantile myofibroma: Clinicopathological and immunohistochemical features of a case series [J]. Acta Histochem, 2015, 117: 431-436.
- [8]Holzer-Fruehwald L, Blaser S, Rossi A, Fruehwald-Pallamar J, Thurnher MM. Imaging findings in seven cases of congenital infantile myofibromatosis with cerebral, spinal, or head and neck involvement [J]. Neuroradiology. 2012, 54: 1389-1398.
- [9]Himori K, Hatori M, Watanabe M, et al. Infantile fibrosarcoma of thigh—a case report [J]. Ups J Med Sci, 2005, 110: 85-93.
- [10]Merrell S C, Rahbar R, Alomari A I, et al. Infantile myofibroma or lymphatic malformation: Differential diagnosis of neonatal cystic cervicofacial lesions [J]. J Craniofac Surg, 2010, 21: 422-426.
- [11]Farmakis S G, Herman T E, Siegel M J. Congenital infantile fibrosarcoma [J]. J Perinatol, 2014, 34: 329-330.
- [12]Sargar K M, Sheybani B F, Shenoy A, et al. Pediatric fibroblastic and myofibroblastic tumors: A pictorial review [J]. RadioGraphics, 2016, 36: 1195-1214.
- [13]Orbach D, Rey A, Cecchetto G, Oberlin O, et al. Infantile Fibrosarcoma: Management based on the European experience [J]. J Clin Oncol, 2010, 28: 318-323.
- [14]Halliday A, Idikio. Quantitative analysis of p53 expression in human normal and cancer tissue microarray with global normalization method. Int J Clin Exp Pathol, 2011, 4 (5): 505-512.
- [15]Li L T, Jiang G, Chen Q, et al. Ki67 is a promising molecular target in the diagnosis of cancer (Review) [J]. Mol Med Rep, 2015, 11 (3): 1566-1572.
- [16]Tong G, Zhang G, Liu J, et al. Cutoff of 25% for Ki67 expression is a good classification tool for prognosis in colorectal cancer in the AJCC-8 stratification. Oncol Rep, 2020, 43 (4): 1187-1198.

(收稿日期: 2021-07-05)

(校对编辑: 阮靖)